Geochimica et Cosmochimica Acta Vol. 51, pp. 623–630

0016-7037/87/$3.00 + .00

Germanium crystal chemistry in hematite and goethite from the Apex Mine, Utah, and some new data on germanium in aqueous solution and in stottite

LAWRENCE R. BERNSTEIN and GLENN A. WAYCHUNAS
Center for Materials Research, Stanford University, Stanford, CA 94305, U.S.A.

(*Received September* 18, 1986; *accepted in revised form December* 5, 1986)

Abstract—At the Apex Mine in southwest Utah, fine-grained hematite contains as much as 1.0 wt. percent Ge, and fine-grained goethite contains as much as 0.7 wt. percent Ge. The mode of Ge incorporation in these minerals was investigated by high-resolution K-edge fluorescence spectroscopy using synchrotron radiation. Analysis of extended fine structure (EXAFS) K-edge data for Ge and Fe shows that Ge substitutes for Fe in the octahedral metal sites of the studied hematite and goethite, with average Ge-ligand bond lengths of 1.88 Å. The solid solution in hematite probably occurs through the coupled substitution 2Fe(III) = Ge(IV) + Fe(II), similar to the coupled substitution 2Fe(III) = Ti(IV) + Fe(II) that occurs in the solid solution series hematite-ilmenite. The solid solution in goethite probably occurs by the loss of an H atom from an OH group, through the coupled substitution Fe(III) + H(I) = Ge(IV). In related experiments, EXAFS data indicate that in a neutral aqueous solution containing 790 ppm Ge, the Ge occurs predominately as $Ge(OH)_4$, with tetrahedral Ge-OH bond lengths of 1.74 Å. In stottite, $FeGe(OH)_6$, Fe(II) and Ge(IV) occur in octahedral sites with average Fe-OH and Ge-OH bond lengths of about 2.20 Å and 1.88 Å.

INTRODUCTION

GERMANIUM OCCURS IN the earth's crust at an average concentration of 1.5 parts per million, primarily as tetrahedral Ge(IV) substituting for tetrahedral Si(IV) in silicate minerals. The element is enriched relative to this average in a wide variety of geologic materials, including coal, iron meteorites, sphalerite, copper-, silver-, and arsenic-rich sulfides, and iron oxides and hydroxides (BERNSTEIN, 1985). The crystal chemistry of germanium in many of these non-silicate materials remains poorly understood. In particular, the modes of germanium incorporation in sphalerite and in some iron oxides and hydroxides (currently the major ores of germanium) are not known. In this study, the incorporation of germanium in hematite and goethite was investigated using high-resolution Ge and Fe K-edge fluorescence data obtained with synchrotron radiation.

Occurrence of Ge in iron oxides and hydroxides

The tendency for germanium to concentrate in iron oxides has been known since the observations of GOLDSCHMIDT and PETERS (1933), who reported 5–100 ppm Ge in samples of hematitic iron ore from several localities. BURTON *et al.* (1959) reported 83 ppm Ge in a sample of hematite from Cumberland, England, though lower concentrations were found in several iron oxide and hydroxide samples from other localities. SCHRÖN (1969) found 260 and 435 ppm Ge in two hematite samples from iron-barite ore at Hora Blatna in Bohemia, Czechoslovakia, and 19.5–39 ppm Ge in three German hematite samples. Many large sedimentary and volcanogenic-sedimentary iron ore deposits in the U.S.S.R. are reported to contain relatively high concentrations of germanium (generally 20–50 ppm, locally reaching 100 ppm Ge; *e.g.* BEKMUKHAMETOV *et al.*, 1973; SAPRYKIN, 1977; VAKHRUSHEV and SEMENOV, 1969; VOSKESENSKAYA *et al.*, 1975). The germanium in these deposits occurs mainly in magnetite, hematite, and goethite.

High germanium concentrations have also been found in some recent iron hydroxide precipitates. GOLDSCHMIDT and PETERS (1933) found 100 ppm GeO_2 in ferric hydroxide precipitates from a hot spring on the island of Volcano, Italy, and GRIGOR'YEV and ZELENOV (1965) found 11–15 ppm Ge in Fe and Mn oxide-hydroxide precipitates collected from submarine hot springs near the Banu-Wuhu volcano, Indonesia.

Apex Mine, Washington County, Utah. At the Apex Mine in southwest Utah, germanium is commercially extracted from fine-grained hematite (as much as 1.0 wt. percent Ge), goethite (as much as 0.7 wt. percent Ge), and "limonite" (poorly crystallized goethite, lepidocrocite, and hematite; as much as 0.5 wt. percent Ge) (BERNSTEIN, 1986). These minerals are the products of the complete supergene oxidation of a steeply dipping copper- and arsenic-rich sulfide body within gently dipping Pennsylvanian limestone. The nature of the germanium associated with these minerals has not been known. The possible sites for germanium in these minerals include: (1) substituting for Fe in crystallographic sites; (2) incorporation in interstitial atomic sites; (3) adsorption on fractures and grain boundaries; and (4) presence of discrete Ge-rich phases, such as GeO_2 (either the quartz- or rutile-structure polymorph), stottite ($FeGe(OH)_6$), or other compounds.

Previous work

A few experimental studies have demonstrated the affinity of germanium for precipitated ferric hydroxides. BURTON *et al.* (1959) found that 95% of dissolved Ge is co-precipitated from seawater with ferric hydroxide. PAZENKOVA (1967) reported that over 90% of dissolved Ge is co-precipitated with ferric hydroxide from water having a pH greater than 6,

whereas less Ge is co-precipitated at lower pH levels. She found most of the Ge to be strongly bound to the ferric hydroxide precipitate, and not weakly adsorbed to it.

Several studies have explored the phase relations in the systems Fe_2O_3-GeO_2-FeO and Fe_2O_3-GeO_2 at 1 bar and 1000°C. TAKAYAMA *et al.* (1981), TAKAYAMA and KIMIZUKA (1981), and MODARESSI *et al.* (1984) studied the larger system, and found the new compounds $Fe_{3.2}Ge_{1.8}O_8$ (modified spinel (βMg_2SiO_4) structure containing Ge_2O_7 groups), $Fe_9Ge_5O_{22}$ (unknown structure), $Fe_4Ge_2O_9$ (unknown structure), and $Fe_{1.07}Ge_{0.93}O_3$ (orthopyroxene structure). TAKAYAMA and KIMIZUKA (1981) reported $FeGeO_3$ to have a clinopyroxene structure. AGAFONOV *et al.* (1984) studied the system Fe_2O_3-GeO_2, and produced large crystals (as much as 1.5 mm) of Fe_2GeO_5 (kyanite structure), $Fe_8Ge_3O_{18}$ (unknown structure, possibly related to kyanite), GeO_2 (rutile structure), and α-Fe_2O_3 (hematite).

The mineral brunogeierite ($GeFe_2O_4$) has a normal spinel structure, with Ge(IV) in the tetrahedral sites and Fe(II) in the octahedral sites. This mineral forms a complete solid solution series with the inverse spinel magnetite (Fe_3O_4), through the coupled substitution Ge(IV) + Fe(II) = 2Fe(III) (OTTEMANN and NUBER, 1972; MODARESSI *et al.*, 1984; TAKAYAMA *et al.*, 1981).

A diagram showing the reported phase relationships in the system Fe_2O_3-GeO_2-FeO at 1000°C is given in Fig. 1. The system is complex, and requires further study.

No systematic studies have been reported on the solubility of germanium in hematite or goethite. AGAFONOV *et al.* (1984) did, however, report that neutron activation analysis detected 1.4 mole percent GeO_2 (1.0 wt. percent Ge) in hematite that they crystallized at 1000°C from an initial mixture of 90 mole percent Fe_2O_3 and 10 mole percent GeO_2.

EXPERIMENTAL MATERIALS AND METHODS

Samples of hematite and goethite from the Apex Mine, Washington County, Utah were investigated. The hematite is from drill hole DDH85-9, 45–47 m, and consists of reddish-brown nodules 5–20 mm across of fine-grained material (<1 μm grain size, based on SEM observation). The goethite is from the same location, consisting of yellow-brown friable nodules 5–30 mm across of fine-grained (<1 μm) material.

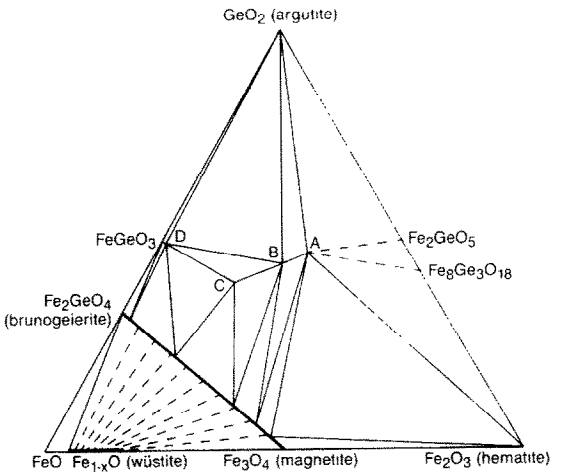

FIG. 1. Phase relations in the system GeO_2-FeO-Fe_2O_3 at 1000°C, adapted from data of TAKAYAMA *et al.* (1981), MODARESSI *et al.* (1984), and AGAFONOV *et al.* (1984). Lettered compounds are: A—$Fe_{3.2}Ge_{1.8}O_8$; B—$Fe_9Ge_5O_{22}$; C—$Fe_4Ge_2O_9$; D—$Fe_{1.07}Ge_{0.93}O_3$. Solid tie-lines are experimentally derived; dashed tie-lines are schematic; heavy lines indicate solid solution.

The Apex hematite and goethite samples were studied by powder X-ray diffraction, using Cu Kα radiation on a Rigaku automated diffractometer with a diffracted beam monochromator at the Department of Geology, Stanford University. The hematite sample gave only peaks for hematite and quartz, and the goethite sample gave only peaks for goethite and quartz. The goethite peaks were broad and weak, indicating a very small crystal size. The full width at half maximum for the 111 goethite reflection at 2θ = 36.65° is 0.41°, compared to 0.28° for the coarsely crystalline goethite from Michigan, indicating an average grain size of about 300 Å for the Apex material. It is possible that other very fine-grained or amorphous iron oxides and hydroxides are also present that do not produce measurable diffraction peaks.

The samples were also examined in a Cambridge Stereoscan scanning electron microscope (SEM) with an energy dispersive X-ray elemental analyzer at the U.S. Geological Survey, Menlo Park, California. The hematite was found to be admixed with microcrystalline (<1 μm) quartz, and sparse scattered grains of plumbian jarosite (2–10 μm). The hematite-quartz mixture contains as much as a couple of percent Ca, K, and Al, suggesting the presence of traces of calcite and clay minerals. Roughly 1 wt. percent As and 0.7 wt. percent Ge were also detected. Within scattered larger quartz grains (>5 μm) no trace elements, including Ge, were detected at the detection limit of about 500 ppm. The goethite sample was very similar, though it contained less sub-micrometer quartz, and more quartz grains larger than 5 μm across. Roughly 1 wt. percent As and 0.2 wt. percent Ge were detected in the goethite. Traces of plumbian jarosite, and possibly calcite and clay minerals, were also observed. No trace elements were detected in the quartz. The concentration of Ge appeared fairly uniform in both the hematite and goethite, and no distinct Ge-rich phases were observed.

Semiquantitative emission spectrographic analyses were performed on these samples by Richard Lerner of the U.S. Geological Survey. The complete analyses were presented by BERNSTEIN (1986; Table 2, samples 3 and 6). The hematite sample was found to contain 0.7 wt. percent Ge and 31 wt. percent SiO_2, and the goethite sample was found to contain 0.2 wt. percent Ge and 36 wt. percent SiO_2. Assuming that no Ge occurs in the quartz (as indicated by the SEM observations above, and the K-edge studies, below), then the hematite itself contains 1.0 wt. percent Ge and the goethite itself contains 0.3 wt. percent Ge.

In connection with the K-edge studies, several model compounds of known compositions and crystal structures were used. These consisted of synthetic GeO_2 (quartz-structure), synthetic GeO_2 (rutile-structure), a single crystal of hematite from Elba, Italy (Stanford #1949A), stottite from Tsumeb, Namibia (Smithsonian #141,174), goethite from the Superior Mine, Marquette, Michigan (Stanford #1830), and lepidocrocite from the Elizabeth Friedberg Mine, Bieber, Hessen, West Germany (Stanford #5717). The identities of the samples were all confirmed by powder X-ray diffraction; the lepidocrocite was found to contain a few percent of goethite. An aqueous solution containing 790 ppm Ge was also used for comparison. This solution was prepared by completely dissolving powdered GeO_2 (quartz-structure) in boiling distilled water and filtering the solution. The concentration of the solution was measured by emission spectroscopy at the U.S. Geological Survey. The pH of the solution was measured as 6.0.

K-edge studies

For the K-edge absorption studies, the samples were finely ground (<30 μm), and the resulting powders were sandwiched between pieces of cellophane tape in cardboard sample holders. All of the prepared samples, except for the stottite, contained about one millimeter thickness of powder. The stottite sample was smaller, consisting of only a thin smear of powder. The aqueous solution was contained in a small polyethylene bag, with a solution thickness of a few millimeters.

Data collection was performed at the Stanford Synchrotron Radiation Laboratory (SSRL) on beam line II-3 during dedicated storage ring operation (3 GeV, 40–80 mA). This beam line contained a computer-controlled Si(111) double crystal monochromator. The beam size on the sample was about 2 × 20 mm. The data were collected in the manner described by WAYCHUNAS *et al.* (1986), using a fluorescence detector with an ionization chamber filled with appropriate gas mixtures to maximize sensitivity to the desired X-ray wavelengths. The detector is mounted at right angles to the incident X-ray beam, and a filter is placed between the sample and the ionization chamber to reduce the amount of K_β radiation (Ga_2O_3 filter for Ge K_β and MnO_2 filter for Fe K_β radiation). A Soller slit assembly between the filter and the ionization chamber reduces the filter fluorescence reaching the chamber.

The data were collected by stepping the monochromator over the energy ranges 10,950–12,050 eV for Ge, and 6950–8050 eV for Fe. Increasing increments of 0.5, 2., 4., and 6. eV were used with increasing energy to produce more equal increments in k-space. One of the monochromator crystals was slightly detuned to reduce the intensity of harmonic X-ray wavelengths reaching the sample. Spectra were obtained on Cu and Fe foils supplied by SSRL for calibration of the Ge and Fe data.

Data reduction. The data were calibrated to the first inflection points of the Cu and Fe foil spectra, which were taken as 8980.3 eV for Cu and 7111.2 eV for Fe. For the near-edge (XANES) data (Figs. 2 and 3, Tables 1 and 2), first and second derivatives of the spectra were calculated; the XANES data given in Tables 1 and 2 are based on the zeroes and minima of these derivatives.

Reduction of the extended fine structure (EXAFS) data was complex, and the methods that were used are described in detail by WAYCHUNAS *et al.* (1986). Briefly, the process is: (1) subtract background fluorescence produced by other atoms in the sample and other shells of the studied atom by fitting a cubic spline polynomial to the pre-edge region, extrapolating the curve over the EXAFS range, and subtracting it from the data; (2) estimate and subtract the post-edge background fluorescence profile (without the EXAFS modulations) using 3-region cubic spline fits and subtracting them from the data; (3) convert the data to k-space, where $k = [0.262(E - E_0)]^{1/2}$, with E being the incident X-ray energy, and E_0 the threshold energy for photoelectron ejection. E_0 is not a well-defined quantity, and, at this stage of data reduction, is set to the energy value at the middle of the main edge-slope. (4) The resulting function, $\chi(k)$, is weighted by k^3 and windowed by a Gaussian function to select the k-range and reduce termination ripples for the (5) Fourier transform, which produces the EXAFS structure function (similar to, but distinct from, a radial distribution function). The atomic distances obtained by the transform incorporate EXAFS phase shifts caused by the absorbing and neighboring atoms (dependent on the types of atoms and the range of k-space selected for the transform). As a result, the transform peaks are shifted from their true physical values. To compensate for these effects, (6) each Fourier peak (representing an atomic shell or closely spaced group of shells surrounding the absorbing atom) is separated and back-transformed, and (7) the resulting function is least-squares fit using backscattering phase factors and scaling factors obtained from model compounds. This fitting gives refined values for the distance (R) to the neighboring shell, the coordination number (CN; related to the amplitude of the function), E_0, and a Debye-Waller factor (σ) that is related to the isotropic structure refinement temperature factor B by the relation $\sigma^2 = B/8\pi^2$.

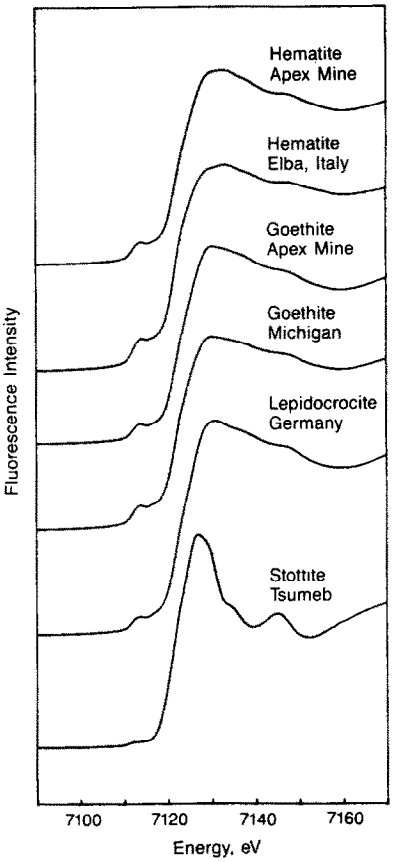

FIG. 3. Near-edge (XANES) spectra for Fe K-edges of several minerals.

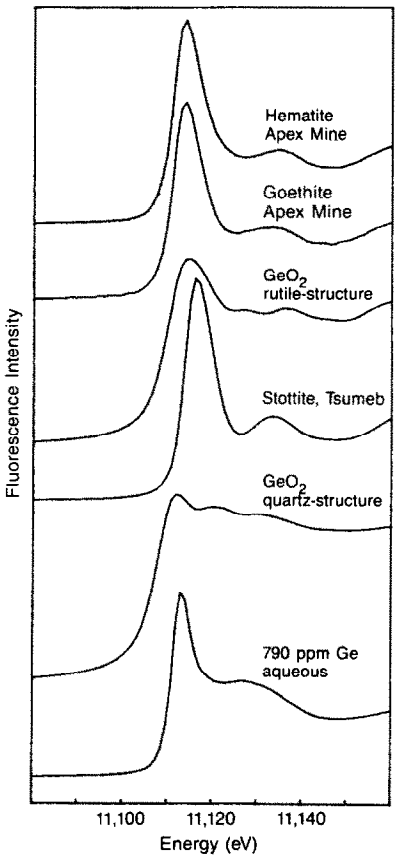

FIG. 2. Near-edge (XANES) spectra for Ge K-edges of several minerals and a dilute aqueous solution.

Table 1. Positions of Ge K-edge XANES features (in eV).

	Edge crest	Post-crest
Hematite, Apex Mine	11,113.7	11,134.9
Goethite, Apex Mine	11,113.6	11,133.3
Stottite, Tsumeb	11,116.2	11,133.5
GeO_2 (rutile)	11,114.6	11,127.1 11,136.3
790 ppm Ge (aqueous)	11,113.0	11,127.0
GeO_2 (quartz)	11,111.8	11,120.2 11,130.8

Estimated standard deviations are 0.1 eV

In this study the range in k-space selected for the Fourier transforms was 4.3–10.5. The range was limited at the upper end by the presence of As in the hematite and goethite from the Apex Mine, which produces a large feature due to the As K-edge at 11,865 eV. Rutile-structure GeO_2 was used as the model compound for the Ge data, and the hematite from Elba, Italy was used as the model compound for the Fe data. Quantitative structural parameters could not be obtained for atomic shells beyond the nearest-neighbor shell in the Apex hematite and goethite, due to the lack of available model compounds containing both octahedral Ge and Fe in a hematite-like or goethite-like structure.

RESULTS

XANES

The Ge K-edge XANES spectra of the investigated materials are shown in Fig. 2, and the numerical data for feature positions are given in Table 1. All of the spectra have a steep initial edge-slope, with no pre-edge features. The hematite, goethite, and GeO_2 (rutile-structure) spectra have edge-crests at 11,113.6–11,114.6 eV. These materials contain Ge in octahedral coordination to O (as discussed below). Stottite, with Ge octahedrally coordinated to OH, has a higher edge-crest energy of 11,116.2 eV. Quartz-structure GeO_2 contains Ge in tetrahedral coordination to O, and has a much lower edge-crest energy of 11,111.8 eV. The dilute aqueous solution produces a spectrum with an edge-crest energy of 11,113.0 eV, which is lower than the values for octahedrally coordinated Ge, but higher than the value for tetrahedral Ge-O coordination. As discussed below, this value probably represents tetrahedral Ge-OH coordination.

The hematite, goethite, and stottite spectra have a single post-crest peak at about 11,134 eV, while the GeO_2 (rutile-structure) spectrum has two peaks centered roughly around 11,132 eV. The GeO_2 (quartz-structure) spectrum has two post-crest peaks at about 11,120 and 11,131 eV, and the dilute aqueous solution has a single peak at about 11,127 eV.

The Fe K-edge XANES spectra (Fig. 3, Table 2) are very similar for the hematite, goethite, and lepidocrocite samples. All have a prominent pre-edge feature at about 7114 eV, which is most intense for hematite. Several other small XANES features are also present. The stottite spectrum has a much smaller pre-edge feature, at 7112.3 eV. The edge-crest is at a lower energy (7127.0 eV), and there are two distinct post-crest XANES features at 7134.2 and 7145.2 eV. The small pre-edge feature and lower edge-crest energy are characteristic of Fe(II) rather than Fe(III) (WAYCHUNAS *et al.*, 1983).

Table 2. Positions of Fe K-edge XANES features (in eV).

	Pre-edge		Edge crest	Post-crest		
Hematite, Apex Mine	7113.9	7123.7	7129.9	7132.9	7138.3	7147.7
Hematite, Elba	7114.1	7123.8	7129.7	7133.1	7138.0	7147.5
Goethite, Apex Mine	7113.8	7123.4	7130.0	7133.8	7137.6	7148.3
Goethite, Michigan	7113.8	7123.4	7130.0	7133.9	7138.0	7147.7
Lepidocrocite, Germany	7113.6	7123.9	7130.6	—	7138.6	7147.5
Stottite, Tsumeb	7112.3	7123.0	7127.0	7134.2	—	7145.2

Estimated standard deviations are 0.1 eV

EXAFS

The EXAFS structure functions for the investigated materials are shown in Figs. 4, 5 and 6. The positions of the peaks in these functions indicate the distances to nearby shells of atoms surrounding the absorbing atom. The sizes of the peaks are related to the numbers and types of neighboring atoms in the shells, as well as to phase interference effects. The distances shown in these figures have not been corrected for phase shifts. Numerical data for the nearest-neighbor atomic shell, corrected for phase shifts using the model compounds, are given in Table 3.

DISCUSSION

The great similarity in the EXAFS structure function curves for Ge and Fe in hematite (Fig. 4) indicates that

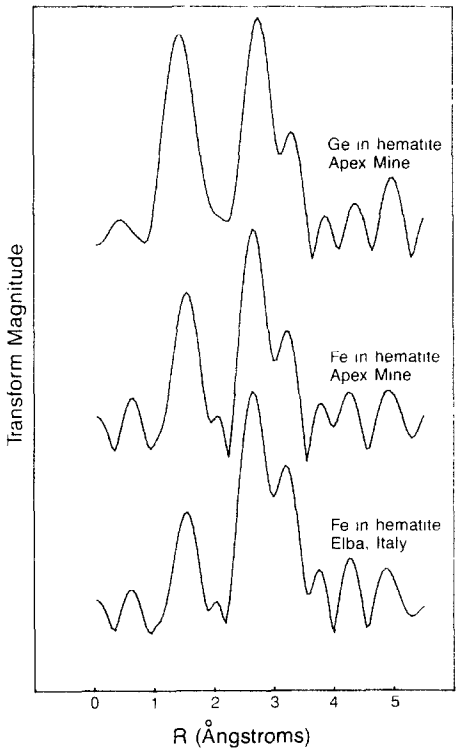

FIG. 4. EXAFS structure functions for Ge and Fe in hematite. These functions are the Fourier transforms of background-subtracted chi-functions of K-edge EXAFS data (see text for details). The radial distances on the figure have not been corrected for photoelectron phase shift effects. Table 1 gives the corrected nearest-neighbor distances.

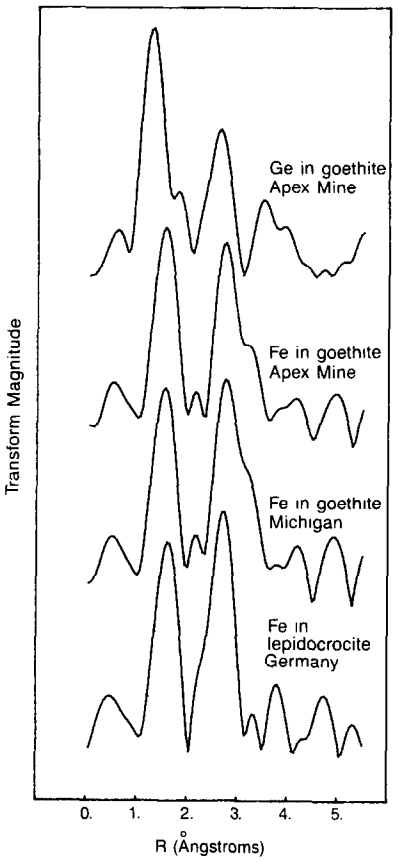

FIG. 5. EXAFS structure functions for Ge in goethite and Fe in goethite and lepidocrocite.

the two elements occur in the same structural site. The phase-shift corrected numerical data (Table 3) show that Ge occurs in octahedral coordination to O, at an average distance of 1.875 Å. This value is typical of an octahedral Ge-O distance (1.8817 Å in rutile-structure GeO_2 (average); HAZEN and FINGER, 1981), and is much larger than for tetrahedrally coordinated Ge (1.739 Å in quartz-structure GeO_2 (average); SMITH and ISAACS, 1964). The curves for Ge in stottite, aqueous solution, and both forms of GeO_2 are seen to differ substantially from that for Ge in hematite, due to the different crystal structures.

The distance represented by the nearest-neighbor peak in hematite (Fig. 4) is clearly smaller for Ge than for Fe, due to the smaller size of Ge(IV) relative to Fe(III). The distances to the outer shells of atoms, however, are very similar for Ge and Fe. This indicates that Ge substitutes for Fe essentially at random, and not in clusters that would significantly distort the local hematite structure.

The EXAFS data for Ge in the goethite sample are somewhat poorer, but strongly indicate that Ge substitutes for Fe in the structure. The lower quality of the data is due mainly to the lower concentration of Ge (and thus weaker X-ray fluorescence), and the fact that the sample probably contains some admixed very fine-grained iron oxides and hydroxides that give diffuse powder X-ray diffraction peaks. The Ge is in an octahedral crystallographic site, coordinated to O and OH at an average distance of 1.879 Å.

The substitution of Ge(IV) for Fe(III) in hematite and goethite requires some type of coupled substitution to maintain valence balance. The simplest concomitant substitution in hematite is Fe(II) for Fe(III) in a nearby octahedral metal site, leading to the coupled substitution 2Fe(III) = Ge(IV) + Fe(II). The similar coupled substitution 2Fe(III) = Ti(IV) + Fe(II) is known to occur in the solid solution series hematite-ilmenite ($FeTiO_3$) (ISHIKAWA and AKIMOTO, 1957; LINDSLEY, 1976). Also, as was mentioned, in the spinels magnetite, $Fe(III)_2Fe(II)O_4$, and brunogeierite, $Ge(IV)Fe(II)_2O_4$, complete solid solution occurs through the coupled substitution 2Fe(III) = Ge(IV) + Fe(II), although the Ge occurs in tetrahedral sites in this case.

The presence of Fe(II) at a level of 1 wt. percent or less, as proposed for the Apex hematite sample, would not produce a detectable signal in the XANES spectrum, due to masking by the Fe(III). The presence of an Fe(II) atom replacing an Fe(III) atom in the second-neighbor shell around a Ge(IV) atom may, however,

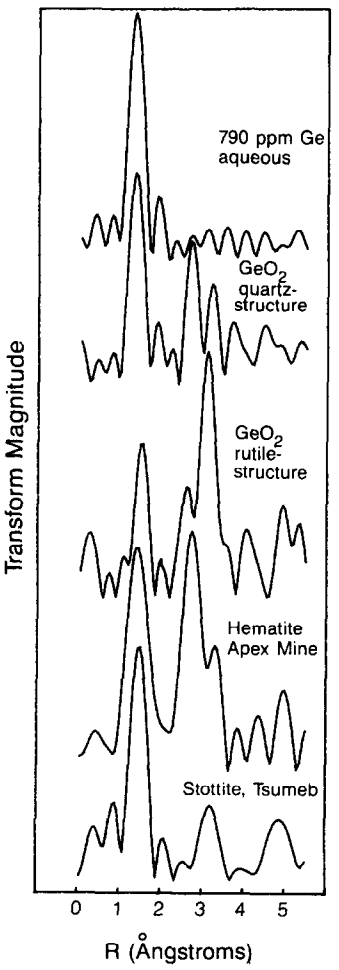

FIG. 6. EXAFS structure functions for Ge in several materials.

Table 3. Parameters derived from EXAFS data for the nearest-neighbor atomic shell.

	Ge K-edge data					
	GeO_2 (rutile)	Hematite Apex Mine	Goethite Apex Mine	Stottite Tsumeb	GeO_2 (quartz)	790 ppm Ge aqueous
R	1.8817*	1.875(2)**	1.879(4)	1.879(2)	1.730(7)	1.736(3)
CN	6.0*	5.2(2)	7.0(4)	5.7(3)	4.0(4)	5.3(3)
σ	0.07	0.08	0.07	0.06	0.05	0.04
E_o	11,110.0	11,109.8	11,109.4	11,107.2	11,110.6	11,108.5

	Fe K-edge data					
	Hematite Elba	Hematite Apex Mine	Goethite Apex Mine	Goethite Michigan	Lepido-crocite	Stottite Tsumeb
R	2.0285*	2.032(2)	2.043(2)	2.044(3)	2.064(2)	2.204(2)
CN	6.0*	5.2(2)	6.0(2)	7.5(3)	6.7(2)	19.0(5)
σ	0.06	0.08	0.09	0.09	0.07	0.06
E_o	7134.0	7134.2	7134.2	7134.2	7134.5	7134.3

Abbreviations: R = average metal-ligand distance in Å; CN = coordination number in atoms; σ = Debye-Waller factor (see text for definition); E_o = threshold energy for photoelectron emission in eV.

*For the model compounds GeO_2 (rutile-structure) and hematite (Elba), these parameters were fixed using crystal structure refinement data. Data for GeO_2 (rutile-structure) from Hazen and Finger (1981), and for hematite from Finger and Hazen (1980).

**Standard deviations in parentheses are only for the curve-fitting. Overall estimated standard deviations are about 0.01 Å for R, 1.0 atom for CN, 0.02 for σ, and 0.8 eV for E_o.

be detectable in the EXAFS structure function, due to the size difference between octahedral Fe(II) (about 0.86 Å) and Fe(III) (about 0.73 Å). (The second-neighbor shell around an iron atom in hematite is composed of four iron atoms at an average distance of 2.95 Å, based on the data of FINGER and HAZEN, 1980). In fact, the peak representing the second-neighbor shell in the upper (Ge) curve of Fig. 4 is displaced slightly to a larger distance relative to the peaks in the lower (Fe) curves. This displacement is consistent with the proposed substitution of Fe(II) for Fe(III) in the second-neighbor shell.

The goethite crystal structure is somewhat more complex than that of hematite, due to the presence of hydrogen. The discussion below uses data from the X-ray and neutron diffraction structure analyses of FORSYTH *et al.* (1968) and SAMPSON (1969). The nearest-neighbor shell around a metal atom in goethite contains three O_1 atoms at an average distance of 1.95 Å, and three O_2 atoms at an average distance of 2.10 Å. The O_2 atoms are closely bonded to H, forming OH groups with the H ions facing away from the metal sites. Two metal atoms are located at distances of 3.02 Å, forming the second-neighbor shell. Where Fe(III) is replaced by Ge(IV) in the structure, valence balance is most simply achieved through the loss of one of the H atoms associated with the O_2 atoms. This coupled substitution can be expressed as Fe(III) + H(I) = Ge(IV). Such a substitution would lead to stronger bonding between the O_2 atom and the adjacent metals, causing slightly shorter average distances to the nearest and second neighbor shells surrounding the Ge(IV). A displacement to shorter distances in the peaks representing these shells is, in fact, observed in Fig. 5.

Coupled substitutions similar to that proposed for the Apex goethite are known to occur in some amphiboles. In oxy-kaersutite, for example, KITAMURA *et al.* (1975) found Ti(IV) to be enriched in the M1 site, in preference to Fe(III), Al(III), Mg(II), and Fe(II). This enrichment is correlated with replacement of OH by O in an adjacent O3 site, resulting in a shortening of the M1-O3 bond length.

The dilute aqueous solution contains Ge having a first-neighbor atomic shell at an average distance of 1.736 Å, consistent with tetrahedral coordination. The calculated coordination number of 5.3 is slightly higher than expected for tetrahedral coordination, even taking into account the experimental errors, and may reflect the presence of higher-coordinated species. Disparities between the structure of the solution and the model compound, and the low concentration of the solution, may, however, have contributed additional errors (as discussed for stottite, below). The XANES data, as mentioned, are somewhat ambiguous, but are consistent with tetrahedral $Ge(OH)_4$ groups. In addition, the pH of the solution (about 6.0) is consistent with the formation of $Ge(OH)_4$ groups in neutral water through the dissociation of water molecules to produce an excess of free H^+ ions. The lack of peaks beyond that for the nearest-neighbor shell (Fig. 6) strongly suggests that no strong complexing or polymerization takes place beyond the $Ge(OH)_4$ groups.

In stottite, Ge and Fe are found to occur in octahedral coordination, based on average Ge-OH and Fe-OH distances of 1.879 Å and 2.204 Å (Table 3). The very high calculated Fe-OH coordination number of 19 (Table 3) probably results from the large structural differences between stottite and the Fe model compound hematite. It is also noted that stottite is the only one of the studied minerals to contain substantial fer-

rous iron. The smaller sample size for stottite compared to all the other samples may have had some influence as well: the smaller sample thickness would produce less scattering and absorption of the beam, and thus a higher ratio of fluorescence intensity relative to the intensity of the incoming beam. For this reason, thin samples are generally expected to produce higher signal to noise ratios for fluorescence data; we plan to test this hypothesis in future experiments.

The Ge-OH and Fe-OH distances observed for stottite differ from those reported by STRUNZ and GIGLIO (1961) in their crystal structure refinement. Their reported average Ge-OH distance of 1.96 Å is much larger than the typical octahedral distance of about 1.88 Å, whereas their average Fe-OH distance of 2.13 Å is substantially smaller than the Fe(II)-O distance of 2.16 Å in FeO, and 2.18 Å in Fe_2SiO_4 (SHANNON, 1976). The sum of the Ge-OH and Fe-OH distances is, however, nearly the same for our work and for that of STRUNZ and GIGLIO (1961). Since the Ge-OH-Fe angle is nearly 180° in the structure proposed by Strunz and Giglio, it is likely that the positions of the metal atoms were correctly determined, but that those of the OH groups are in error. This would not be unusual for a structure refined on the basis of two-dimensional Patterson maps. In addition, the *R* (reliability) factors obtained by Strunz and Giglio are rather large (13–21%) for such a simple structure. This is consistent with erroneous positions for the OH groups.

CONCLUSIONS

1. High-resolution studies of germanium and iron K-edges by EXAFS and XANES spectroscopy using synchrotron radiation show that germanium can substitute for iron in the octahedral metal site of hematite, with an average Ge-O distance of about 1.88 Å. The investigated sample, from the Apex Mine in southwest Utah, contains about 1.0 wt. percent Ge in solid solution. The solid solution probably occurs through the coupled substitution 2Fe(III) = Ge(IV) + Fe(II). This coupled substitution is similar to the coupled substitution 2Fe(III) = Ti(IV) + Fe(II) in the solid solution series hematite-ilmenite.

2. The same experimental methods indicate that germanium can substitute for iron in the octahedral metal site of goethite, with an average Ge-O or -OH distance of about 1.88 Å. Valence balance is probably maintained by the concomitant loss of an H atom from an OH group, through the relation Fe(III) + H(I) = Ge(IV). The investigated sample, from the Apex Mine, contains about 0.3 wt. percent Ge in solid solution.

3. In a neutral aqueous solution containing 790 ppm Ge, the Ge appears to occur predominately as $Ge(OH)_4$, with an average tetrahedral Ge-OH bond length of about 1.74 Å.

4. In the mineral stottite, $FeGe(OH)_6$, Fe(II) and Ge(IV) occur in octahedral sites with average Fe-OH and Ge-OH bond lengths of about 2.20 Å and 1.88 Å. These lengths are reasonable for these ion-ligand pairs, but differ substantially from those reported in a previous crystal structure refinement, suggesting the need for a reinvestigation of the structure.

5. The substantial solubility of germanium in hematite and goethite suggests that these common minerals may host high germanium concentrations at other localities (a few such cases are known from the literature). Analyses are being conducted for germanium on numerous iron oxide and hydroxide samples to explore this possibility.

Acknowledgements—This work was supported by the NSF-MRL Program through the Center for Materials Research at Stanford University. We thank the Smithsonian Institution, through the courtesy of Pete J. Dunn, for supplying the stottite sample; Wayne A. Dollase (UCLA) for supplying the quartz-structure GeO_2 sample; and Musto Explorations Ltd. (Vancouver, Canada) for use of samples from the Apex Mine.

Editorial handling: R. G. Burns

REFERENCES

AGAFONOV V., MICHEL D., PEREZ Y JORBA M. and FEDOROFF M. (1984) Chemical and crystallographic characterization of crystals grown by chemical vapour transport in the Fe_2O_3-GeO_2 system. *Mater. Res. Bull.* **19,** 233–239.

BEKMUKHAMETOV A. E., ZAMYATINA G. M. and KALININ S. K. (1973) Geochemistry of germanium in the iron deposits of Kazakhstan. *Geochem. Internat.* **10,** 277–282.

BERNSTEIN L. R. (1985) Germanium geochemistry and mineralogy. *Geochim. Cosmochim. Acta* **49,** 2409–2422.

BERNSTEIN L. R. (1986) Geology and mineralogy of the Apex germanium-gallium mine, Washington County, Utah. *U.S. Geol. Surv. Bull. 1577,* 9 p.

BURTON J. D., CULKIN F. and RILEY J. P. (1959) The abundances of gallium and germanium in terrestrial materials. *Geochim. Cosmochim. Acta* **16,** 151–180.

DURIF-VARAMBON A., BERTAUT E. F. and PAUTHENET R. (1956) Étude des germanates spinelles. *Ann. Chem. (Paris)* **13,** 525–543.

FINGER L. W. and HAZEN R. M. (1980) Crystal structure and isothermal compression of Fe_2O_3, Cr_2O_3, and V_2O_3 to 50 kbars. *J. Appl. Phys.* **51,** 5362–5367.

FORSYTH J. B., HEDLEY I. G. and JOHNSON C. E. (1968) The magnetic structure and hyperfine field of goethite (α-FeOOH). *J. Phys. C,* ser. 2, 1, 179–188.

GOLDSCHMIDT V. M. and PETERS C. (1933) Zur Geochemie des Germaniums. *Nach. Ges. Wiss. Göttingen, Math.-Phys. Kl., Fachgruppe III,* no. 31, 141–166.

GRIGOR'YEV V. M. and ZELENOV K. K. (1965) On the source of germanium in iron ores. *Geochem. Internat.* **2,** 445–448.

HAZEN R. M. and FINGER L. W. (1981) Bulk moduli and high-pressure crystal structures of rutile-type compounds. *J. Phys. Chem. Solids* **42,** 143–151.

ISHIKAWA Y. and AKIMOTO S. (1957) Magnetic properties of the $FeTiO_3$-Fe_2O_3 solid solution series. *J. Phys. Soc. Japan* **12,** 1083–1098.

KITAMURA M., TOKONAMI M. and MORIMOTO N. (1975) Distribution of titanium atoms in oxy-kaersutite. *Contrib. Mineral. Petrol.* **51,** 167–172.

LINDSLEY D. H. (1976) The crystal chemistry and structure of oxide minerals as exemplified by the Fe-Ti oxides. In *Oxide Minerals* (ed. D. RUMBLE, III), *Reviews in Mineralogy,* vol. 3, pp. L1–L60. Mineralogical Society of America.

MODARESSI A., GERARDIN R., MALAMAN B. and GLEITZER C. (1984) Structure et propriétés d'un gérmanate de fer de valence mixte $Fe_4Ge_2O_9$. Etude succincte de $Ge_xFe_{3-x}O_4$ ($x \leq 0.5$). *J. Solid State Chem.* **53,** 22–34.

OTTEMANN J. and NUBER B. (1972) Brunogeierit, ein Germanium-Ferritspinell von Tsumeb. *N. Jb. Mineral. Mh.* **1972,** 263–267.

PAZENKOVA N. I. (1967) Germaniferous limonite-forming mechanism. *Dok. Acad. Sci. U.S.S.R., Earth Sci. Sect.* **173,** 204–206. (English translation).

ROSSITER M. J. (1966) Mössbauer absorption in some ferrous spinels. *Phys. Lett.* **21,** 128–130.

SAMPSON C. F. (1969) The lattice parameters of natural single crystal and synthetically produced goethite (α-FeOOH). *Acta Cryst.* **B25,** 1683–1685.

SAPRYKIN F. YA. (1977) Deposits of germanium. In *Ore Deposits of the U.S.S.R.*, vol. 3, (ed. V. I. SMIRNOV), pp. 455–462. Pitman, London.

SCHRÖN W. (1969) Zur Geochemie des Germaniums. II. Lagerstätten genetische Probleme. *Freiberger Forschungshefte* **246,** 5–65.

SHANNON R. D. (1976) Systematic studies of interatomic distances in oxides. In *The Physics and Chemistry of Minerals and Rocks* (ed. R. G. J. STRENS), pp. 403–431. Wiley, New York.

SMITH G. S. and ISAACS P. B. (1964) The crystal structure of quartz-like GeO_2. *Acta Cryst.* **17,** 842–846.

STRUNZ H. and GIGLIO M. (1961) Die Kristallstruktur von Stottit, $Fe[Ge(OH)_6]$. *Acta Cryst.* **14,** 205–208.

TAKAYAMA E. and KIMIZUKA N. (1981) Powder x-ray study on iron-germanium pyroxenes. *J. Solid State Chem.* **39,** 262–264.

TAKAYAMA E., KIMIZUKA N., KATO K., YAMAMURA H. and HANEDA H. (1981) The system GeO_2-FeO-Fe_2O_3 at 1000°C. *J. Solid State Chem.* **38,** 82–86.

VAKHRUSHEV V. A. and SEMENOV V. N. (1969) Distribution of germanium in magnetite of iron-ore deposits in the Altai-Sayan region and the Yenisey Ridge. *Geochem. Internat.* **6,** 567–573.

VOSKRESENSKAYA N. Y., VEYMARN A. B. and VINOGRADOVA N. A. (1975) Thallium and germanium in the manganese and iron ores of the Dzhezdy type deposits (central Kazakhstan). *Geochem. Internat.* **12,** 34–39.

WAYCHUNAS G. A., APTED M. J. and BROWN G. E. JR. (1983) X-ray K-edge absorption spectra of Fe minerals and model compounds: near-edge structure. *Phys. Chem. Minerals* **10,** 1–9.

WAYCHUNAS G. A., BROWN G. E. JR. and APTED M. J. (1986) X-ray K-edge absorption spectra of Fe minerals and model compounds: II. EXAFS. *Phys. Chem. Minerals* **13,** 31–47.